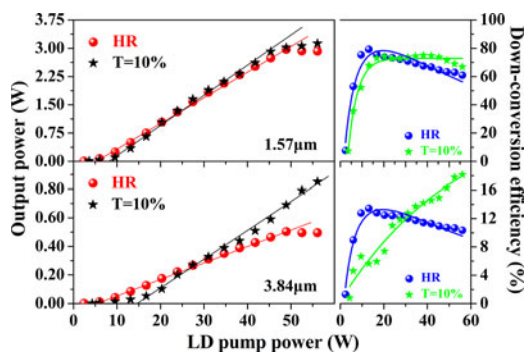


Continuous-Wave Intracavity Multiple Optical Parametric Oscillator Using an Aperiodically Poled Lithium Niobate Around 1.57 and 3.84 μm

Volume 9, Number 2, April 2017

Yongji Yu
Xinyu Chen
Libo Cheng
Shutao Li
Chunting Wu
Yuan Dong
Yuegang Fu
Guangyong Jin



DOI: 10.1109/JPHOT.2017.2657746
1943-0655 © 2017 IEEE

Continuous-Wave Intracavity Multiple Optical Parametric Oscillator Using an Aperiodically Poled Lithium Niobate Around 1.57 and 3.84 μm

Yongji Yu,¹ Xinyu Chen,¹ Libo Cheng,² Shutao Li,¹ Chunting Wu,¹ Yuan Dong,¹ Yuegang Fu,³ and Guangyong Jin¹

¹Jilin Key Laboratory of Solid Laser Technology and Application, School of Science, Changchun University of Science and Technology, Changchun 130022, China

²Department of Engineering Mathematics Basic Teaching, School of Science, Changchun University of Science and Technology, Changchun 130022, China

³Department of Optical Engineering, School of OptoElectronic Engineering, Changchun University of Science and Technology, Changchun 130022, China

DOI:10.1109/JPHOT.2017.2657746

1943-0655 © 2017 IEEE. Translations and content mining are permitted for academic research only.

Personal use is also permitted, but republication/redistribution requires IEEE permission.

See http://www.ieee.org/publications_standards/publications/rights/index.html for more information.

Manuscript received December 7, 2016; revised January 18, 2017; accepted January 19, 2017. Date of current version February 23, 2017. This work was supported in part by the National Natural Science Foundation of China under Grant 61505013 and Grant 61240004, in part by the Postdoctoral Science Foundation of China (2016M591466), and in part by the Science and Technology Department Project of Jilin Province (20150520103JH). Corresponding author: G. Jin (e-mail: yyjcust@163.com).

Abstract: A continuous-wave 1.57 and 3.84 μm intracavity multiple optical parametric oscillator based on a single MgO:APLN crystal is reported for the first time. The synchronized dual-wavelength laser is obtained by using a folded-type double cavity, which consists of a 1064-nm resonator and a multiple optical parametric oscillator. With $T = 10\%$ at 1.47 and 3.3 μm output couplers, maximum output powers of 3.13 W at 1.57 μm and 0.85 W at 3.84 μm are obtained, corresponding to slope efficiencies of 6.8% and 1.9%, respectively. The power stabilities are better than 1.8% and 3% at the maximum output power in half an hour.

Index Terms: Multiple optical parametric oscillator, aperiodically poled lithium niobate, 1.57 μm and 3.84 μm lasers.

1. Introduction

The laser wavelengths operating at approximately 1.57 μm and 3.84 μm belong to the eye-safe wavebands and strong absorption wavebands of the mid-infrared detector, respectively. Owing to their several military applications such as military target range, military countermeasures, and remote monitoring of the special environment, the two-band laser sources have attracted much interest from researchers [1]–[4]. Quasi-phase matching (QPM) optical parametric oscillator (OPO) device with a periodically inverted structure of nonlinear coefficient can enable an efficient wavelength conversion at arbitrary wavelength in the transparent range of the QPM material [5]–[9]. In QPM, the accumulated phase mismatch is offset by modulating the second-order nonlinear coefficient (d_{33}) at a period that is twice the coherence length. Among the QPM materials, MgO-doped congruent lithium niobate (LN) shows relatively high nonlinearity ($d_{33} \sim 25.2 \text{ pm/V@ } 1.064 \mu\text{m}$) with

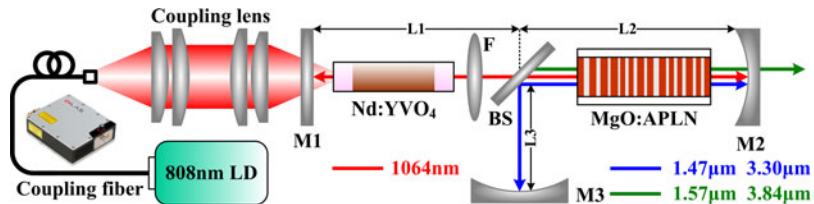


Fig. 1. Schematic diagram of experiment setup.

a wide transparency range ($0.35\text{--}5\ \mu\text{m}$), good optical quality, and mechanical robustness. Owing to these advantages, using a periodically poled MgO:LN (MgO:PPLN) for QPM, various MgO:PPLN-OPOs pumped by a conventional $1.064\ \mu\text{m}$ laser source can be produced using $1.57\ \mu\text{m}$ and $3.84\ \mu\text{m}$ lasers, and proficient results can be obtained [10]–[13]. However, as the primary parametric process converts the pump wave ($\lambda_p \sim 1.064\ \mu\text{m}$) to an idler wave (λ_i) and a resonant signal wave (λ_s), this nonlinear parametric generation essentially relies on energy conservation and momentum conservation, i.e., the $1.57\ \mu\text{m}$ and $3.84\ \mu\text{m}$ laser generation corresponding to two OPO processes, $1.064\ \mu\text{m} \rightarrow 3.3\ \mu\text{m} + 1.57\ \mu\text{m}$ and $1.064\ \mu\text{m} \rightarrow 3.84\ \mu\text{m} + 1.47\ \mu\text{m}$, so that the use of single MgO:PPLN cannot simultaneously phase match both the $1.57\ \mu\text{m}$ and $3.84\ \mu\text{m}$. The two wavelengths can be achieved by cascading two MgO:PPLN crystals inside to the OPO cavity for the two OPO processes [14], [15]. However, high pump depletion in the first crystal, generating the first signal–idler pair, can deteriorate the quality of the pump beam available for the succeeding crystal. This affects the overall OPO performance in terms of the threshold and output power in the second signal–idler pair, thereby causing a low conversion efficiency in the two-step process, and the presence of the second crystal increases the system complexity.

In the previous work, we designed an aperiodically poled MgO:LN (MgO:APLN) domain structure for two-phase mismatch compensation for the $1.57\ \mu\text{m}$ and $3.84\ \mu\text{m}$, and simultaneous high repetition rate pulse generation of dual wavelengths at $1.57\ \mu\text{m}$ and $3.84\ \mu\text{m}$ was obtained by using Q-switched $1.064\ \mu\text{m}$ laser extra-cavity pumping [16]. For this extra-cavity structure, with more rugged structure, easier design, and freedom from relaxation oscillation, however, CW output power could reach multi watts, and pump depletion could exceed 90% when pumped sufficiently far above threshold. In addition, it has a lower efficiency owing to the fact that primary pump laser cannot be recycled. By exploiting the high circulating pump intensities, the intracavity pumping technique uniquely allows extension of the operation of CW OPO to miniature, low-threshold, high efficiency, and the stable operation can be achieved without the need for cavity-length control, which are not attainable with alternative external pumping technique. In this study, we report the synchronized generation of CW $1.57\ \mu\text{m}$ and $3.84\ \mu\text{m}$ intracavity multiple OPO based on the MgO:APLN crystal. Optimizing the intracavity structure and resonant wave output coupling, the maximum output powers at $1.57\ \mu\text{m}$ and $3.84\ \mu\text{m}$ are $3.13\ \text{W}$ and $0.85\ \text{W}$, respectively. The corresponding slope efficiencies are 6.8% and 1.9%, with power stabilities better than 1.8% and 3%, respectively. To the best of our knowledge, this is the first time CW $1.57\ \mu\text{m}$ and $3.84\ \mu\text{m}$ wavelength laser operation has been achieved using a single crystal.

2. Experimental Setup

The experimental setup of the intra-cavity multiple OPO based on single MgO:APLN is shown schematically in Fig. 1. The pumping source is a 808 nm laser diode (LD) array module of DILAS Corp. by fiber-coupled, which has a maximum power of $56\ \text{W}$ at the output of a $400\ \mu\text{m}$ 0.22 numerical aperture fiber. In our experiments, the a-cut adhesive-free bond composite Nd:YVO₄ crystal ($3 \times 3 \times 24\ \text{mm}^3$) at $1.064\ \mu\text{m}$ is used as the gain medium. It consists of three separate sections, i.e., a $16\ \text{mm}$ 0.25% Nd³⁺-doped YVO₄ sandwiched by two $4\ \text{mm}$ undoped YVO₄ and both ends of the crystal are antireflection (AR) coated at 808 and 1064 nm. In order to decrease the

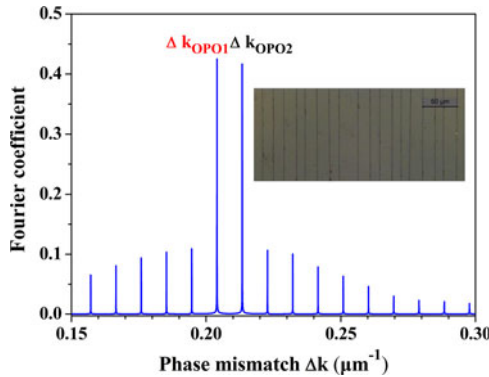


Fig. 2. Fast Fourier transform of the designed MgO:APLN domain structure. (Inset) Microscopic image of the crystal surface (Leica DMI5000M).

influence of the thermal effects, the crystal is wrapped with indium foil and mounted in a red copper holder cooled at 20 °C by refrigerant water. The pump beam from the fiber is imaged into the gain medium with 1:1.5 ratio coupling lenses. M1 is a K9 plano mirror which is highly transmittance (HT) coated at 808 nm ($T > 99\%$) and highly reflectance (HR) coated at 1064 nm ($R > 99.9\%$). M2 is a CaF₂ concave mirror with 100 mm radius of concave (ROC), which is HR coated at 1064 nm ($R > 99.9\%$) and HT coated at 1.5–1.7 μm and 3.7–4.2 μm ($T > 97\%$). M2 constitutes the 1064 nm laser oscillating sub-cavity along with M1. The multiple OPO sub-cavity consists of M2, a CaF₂ plano mirror beam splitter (BS), which is HT coated at 1064 nm ($T > 96\%$) on both sides and HR coated at 1.4–1.7 μm and 3.1–4.2 μm ($R > 99.8\%$ with 45°) on the right-hand side, and a CaF₂ concave mirror (ROC = 100 mm) M3, which is HR coated at 1064 nm, 1.4–1.7 μm , and 3.1–4.2 μm ($R > 99.8\%$). To investigate the influence of multiple OPO resonant wave output coupling, output mirror M2, which is coated two different transmittances with HR and $T = 10\%$ for both of 1.4–1.5 μm and 3.1–3.4 μm . The entire double cavity shares a common M2 mirror and is separated by a BS.

A 5% MgO-doped APLN crystal with dimensions of 50 × 6 × 1 mm^3 , for which both the ends of the faces are AR coated at 1064 nm, 1.4–1.7 μm , and 3.3–4.2 μm , is applied as the nonlinear medium. We designed the MgO:APLN domain structure using the simulated annealing (SA) method [17], [18], which provides double reciprocal vectors to compensate for the phase mismatches for the 1.57 μm and 3.84 μm . Using the Sellmeier equation of Paul *et al.* [19], we calculated the phase mismatches of $\Delta k_{\text{OPO1}} = 0.2041 \mu\text{m} - 1$ @ 1.57 μm and $\Delta k_{\text{OPO2}} = 0.2135 \mu\text{m} - 1$ @ 3.84 μm at room temperature. Considering the fabrication restraints, the MgO:APLN parameters are set as follows: the smallest unit of the domain is 5 μm , and the total length of the crystal is 50 mm. The optimal consecutive order of the domains is obtained by choosing the appropriate objective function in the SA method. From the fast Fourier transform of the final designed MgO:APLN domain structure shown in Fig. 2, the Fourier coefficients related to the two OPO processes were obtained as 0.42 and 0.41, respectively. Higher and approximately equal Fourier coefficient for the two OPO processes, which can be improved the conversion efficiencies and made maximum to balance the gain of the two OPO processes. During the experiment, the MgO:APLN crystal is placed in a servo-controlled oven (HCP Corp.) whose temperature is kept working at room temperature with an accuracy of ± 0.1 K.

Through a high precision-bounded stable cavity method [20], the thermal focal length of the Nd:YVO₄ crystal is measured to be 155 mm under the maximum LD pump power. In order to maintain the thermal stability of the entire pump range and increase the 1064 nm laser pump intensities in the MgO:APLN crystal, a focusing lens F with a focal length of 150 mm utilized as an optical ballast can make the 1064 nm laser beam radius insensitive to thermal lens effects and focus the 1064 nm laser waist radius for the purpose of ensuring sufficient pump intensity. It is located close to the Nd:YVO₄ crystal. The 1064 nm laser oscillate sub-cavity length (M1–M2) is

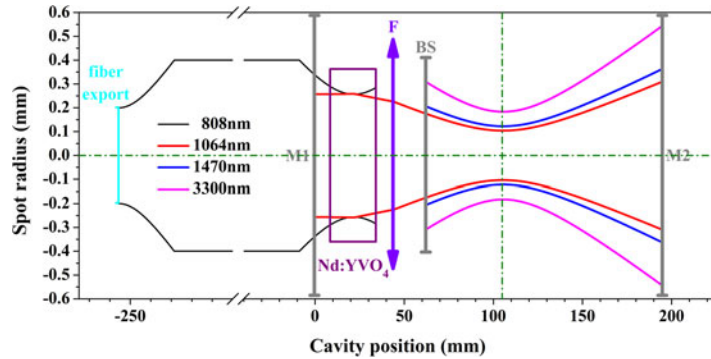


Fig. 3. Simulated beam transmission in the entire cavity of different wavelength lasers.

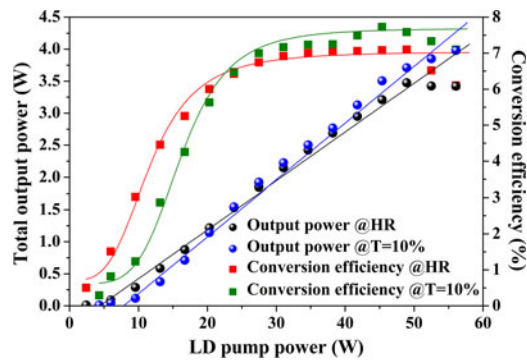


Fig. 4. Total output power and corresponding optical-optical conversion efficiency versus LD pump power.

set to 195 mm, and the BS is placed 62 mm away from M1 (i.e., L₁ = 62 mm, L₂ = 133 mm). As a result, the 1064 nm TEM₀₀ mode laser beam radius in the Nd:YVO₄ crystal is 265 μm , which matched the 300 μm pump spot radius well. Meanwhile, the beam waist radius of the 1064 nm laser is narrowed to 104 μm and appeared at 89 mm from M2. A proficient spatial overlapping is achieved in both processes of the 1064 nm laser and multiple OPO, thus ensuring a high conversion efficiency. Simultaneously, the focusing parameters of the 1064 nm laser and multiple OPO resonant wave agreed well reducing the diffraction loss. The focusing parameters $\xi = L/b$, where L is the MgO:APLN crystal length, and b is the confocal parameters according to the following equations $b = 2\pi n \omega^2/\lambda$. Here, n is the refractive index of the MgO:APLN crystal, ω is the laser beam waist radius, and λ is the wavelength of the laser. The multiple OPO sub-cavity length (M2–M3) is set to 178 mm, and BS is 45 mm away from M3 (i.e., L₃ = 45 mm). In this case, ABCD beam transfer matrix is used to calculate the ray tracing in the entire cavity (M1–M2), and it is shown in Fig. 3. The beam waist radii of the 1.47 μm and 3.3 μm resonant waves are narrowed to 124 μm and 184 μm , respectively, and both appeared at 89 mm from M2. Corresponding to the focusing parameters of the 1064 nm laser, 1.47 μm and 3.3 μm resonant wave are $\xi_{1064\text{nm}} = 0.3667$, $\xi_{1.47\mu\text{m}} = 0.3675$ and $\xi_{3.3\mu\text{m}} = 0.3769$, respectively. Well mode matching is achieved in both processes of lasing and multiple parametric oscillation.

3. Results and Discussion

With this configuration, we first measure the total output power of this laser's operation at dual wavelengths by using output mirror M2 with HR and T = 10%. Fig. 4 shows the total output power (measured by a power meter: OPHIR F150A-BB-26-PPS) and corresponding optical-optical

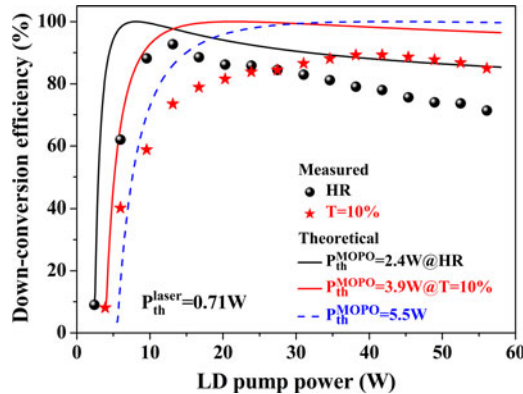


Fig. 5. 1064-nm parent laser down-conversion efficiencies with different output coupler transmittances versus LD pumped power.

conversion efficiency as a function of LD pump power. As can be seen, the multiple OPO threshold (P_{th}^{MOPD}) increases from 2.4 W with the HR output coupler to 3.9 W with $T = 10\%$. When using the HR output coupler, a maximum output power of 3.47 W is obtained under LD pump power of 49 W (absorption efficiency $\sim 89\%$), corresponding to an optical–optical conversion efficiency of 7.1%. Using an output coupling of 10% compared with HR, the maximum output power increases to 3.98 W under the maximum LD pump power of 56 W, but the corresponding optical–optical conversion efficiency decreases from 7.6% with LD pump power of 49 W to 6.6%. It is worth pointing out that when the LD pump power is less than 49 W, both the output power increase rapidly as the LD pump power, the conversion efficiency are tending to maximize under LD pump power of 49 W, but when the LD pump power is higher than 49 W, both the output power started to deviate from the linear increase by contrast due to the serious thermal effect in the Nd:YVO₄ crystal. Moreover, in this range, which is the thermal stability of the pump, the output power and the corresponding optical–optical conversion efficiency increase rapidly with the increase in the threshold owing to higher resonant wave output coupling transmittance. According to the measured the total output power with different output coupling, the frequency down-conversion power of the 1064 nm parent laser is calculated using the relation $P_{DC} = (2P_j/\eta)/(λ_p/λ_j)$ in [21], where the factor of 2 accounts for the two-way propagation, and η is the 1.57 μm and 3.84 μm laser output coupling efficiency, as shown in Fig. 5.

When using the HR output coupler, the down-conversion efficiency increases rapidly after exceeding a threshold of 2.4 W and reaches a maximum value of 93% under LD pump power of 13 W, and then gradually reduces to 71%. This process can be regarded as an energy back-flow at 1064 nm parent laser, which can be called back conversion. When it turns to the $T = 10\%$, the maximum down-conversion efficiency is 89% under LD pump power of 42 W, and no obvious back conversion in the full range of LD pump power. According to the CW intra-cavity OPO theory [22], the theoretical down-conversion efficiencies under different thresholds are calculated based on the measured 1064 nm parent laser threshold (P_{th}^{laser}) of 0.71 W, respectively. The variation trend of measured values are basically consistent with that of theoretical values at HR and $T = 10\%$, as shown in Fig. 5, the two measured values lower than theoretical values owing to the degeneration of beam quality induced by thermal effect aggravation. Both theory simulation and experimental results show that increasing the multiple OPO threshold can suppress the back conversion. Such as increases the threshold power to 5.5 W in theoretical, which lead to less efficiency decline under high pump power.

Using a beam-splitting system with two split mirrors, one of split mirrors which is HT coated at 1.5–1.7 μm and 3.7–4.2 μm and HR coated at 1.4–1.5 μm and 3.1–3.4 μm with 45°, another which is HT coated at 3.1–4.2 μm and HR coated at 1.4–1.7 μm with 45°, we obtained the two synchronized output spectrums and individual output powers. Fig. 6 shows the measured output

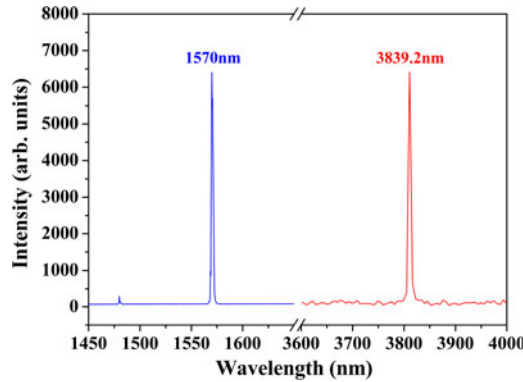
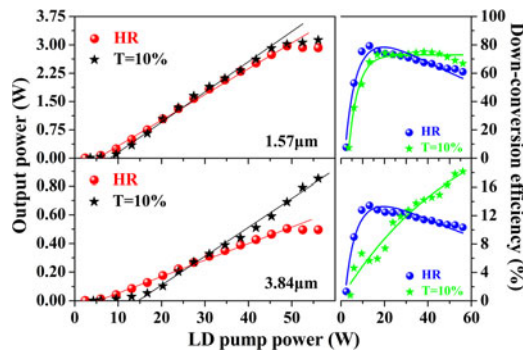


Fig. 6. Measured output spectrums of the multiple OPO.

Fig. 7. $1.57 \mu\text{m}$, $3.84 \mu\text{m}$ output power and corresponding 1064-nm parent laser down-conversion efficiencies with different output coupler transmittances versus LD pumped power.

spectrums of dual-wavelength laser at the maximum output power with HR mirror as M2. The two peak wavelengths are located at 1570 nm (measured by a YOKOGAWA AQ6375 optical spectrum analyzer with a spectral range of 1.2–2.4 μm) and 3839.2 nm (measured by a ARCoptix FTIR-C-20-1203 infrared Fourier spectrometer with a spectral range of 2.5–12 μm), with the spectral linewidths of 2.5 nm and 7.1 nm, respectively. With the pump power increases from 20 W to 56 W, the $1.57 \mu\text{m}$ and $3.84 \mu\text{m}$ emission linewidths increase from 1.1 to 2.5 nm, 3.2 to 7.1 nm, respectively. There is an apparent increase in the spectral linewidth caused by high gain when increasing the pump power.

Fig. 7 shows the output power of $1.57 \mu\text{m}$ and $3.84 \mu\text{m}$ lasers as a function of LD pump power for the two output coupler transmissions. As is shown in Fig. 7, the $1.57 \mu\text{m}$ and $3.84 \mu\text{m}$ laser thresholds increase from 2.4 to 3.9 W and 2.7 to 4.5 W with the increasing of the resonant wave output coupler transmissions, and the laser output powers increase almost linearly with the pump powers. Using HR, the maximum output powers of 2.97 W at $1.57 \mu\text{m}$ and 0.5 W at $3.84 \mu\text{m}$ are obtained. With an output coupling of 10%, the maximum output powers of 3.13 W at $1.57 \mu\text{m}$ and 0.85 W at $3.84 \mu\text{m}$ are obtained, corresponding to slope efficiencies of 6.8% and 1.9%, respectively. In comparison to the HR, the output power and extraction efficiency can be further increased, especially at the $3.84 \mu\text{m}$ waveband, the improvement is more apparent. To take a comparison, the $1.57 \mu\text{m}$ and $3.84 \mu\text{m}$ output power corresponding down-conversion efficiencies has the same trendline of change when using HR output coupling. However, the $3.84 \mu\text{m}$ down-conversion efficiencies with $T = 10\%$ kept rising and were shown to be different from the changing trends, which means that the multi-OPO with two pairs of parametric fields does not follow the cited steady-state power model, owing to the competition between the two OPOs gain, and are

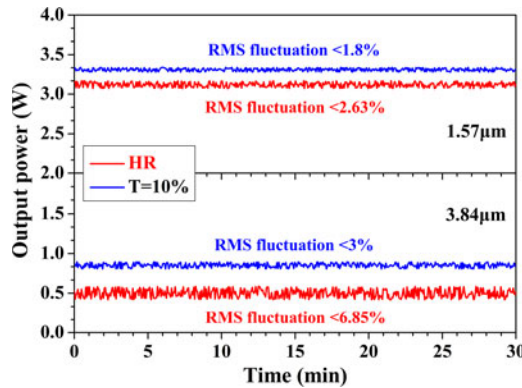


Fig. 8. $1.57\text{ }\mu\text{m}$, $3.84\text{ }\mu\text{m}$ output power stability with different output coupler transmittances as a function of time.

quite different with a common OPO with only one pair of signal and idler. Because the repressed of back conversion and the reduction of gain competition by increasing the transmittance of resonant wave, the Root Mean Square (RMS) fluctuation of the maximum output power with $T = 10\%$ are 1.8% at $1.57\text{ }\mu\text{m}$ and 3% at $3.84\text{ }\mu\text{m}$, respectively, over 30 min under free-running conditions, as shown in Fig. 8. They are much better than the 2.63% RMS fluctuation at $1.57\text{ }\mu\text{m}$ and 6.85% RMS fluctuation at $3.84\text{ }\mu\text{m}$ under using HR. In particular, the imbalance proportion of the output power at $1.57\text{ }\mu\text{m}$ and $3.84\text{ }\mu\text{m}$ as a result of the same transmittance of resonant waves at $3.3\text{ }\mu\text{m}$ and $1.47\text{ }\mu\text{m}$ needs to be further optimized in subsequent studies.

4. Conclusion

In conclusion, we have demonstrated a CW intracavity multiple OPO based on single MgO:APLN crystal, which can provide two-phase mismatch compensations. With $T = 10\%$ output coupler, the maximum output powers of 3.13 W at $1.57\text{ }\mu\text{m}$ and 0.85 W at $3.84\text{ }\mu\text{m}$ are obtained simultaneously, and the corresponding slope efficiencies are 6.8% and 1.9% , respectively. Meanwhile, the maximum output power stabilities are better than 1.8% at $1.57\text{ }\mu\text{m}$ and 3% at $3.84\text{ }\mu\text{m}$, respectively. The experimental results indicate that the compact intracavity multiple OPO operation opens a new door for the synchronized generation of CW $1.57\text{ }\mu\text{m}$ and $3.84\text{ }\mu\text{m}$ laser. Furthermore, the transmittance of the resonant wave is optimized to balance the dual-wavelength power ratio, which makes it an attractive source for practical applications.

References

- [1] K. N. Gorbachenya *et al.*, "Eye-safe $1.55\text{ }\mu\text{m}$ passively Q-switched Er, Yb:GdAl₃(BO₃)₄ diode-pumped laser," *Opt. Lett.*, vol. 41, no. 5, pp. 918–921, 2016.
- [2] X. Ding *et al.*, "Efficient eye-safe Nd:YVO₄ self-Raman laser in-band pumped at 914 nm," *IEEE Photon. J.*, vol. 7, no. 6, Dec. 2015, Art. no. 1503807.
- [3] M. Bernier, V. Fortin, M. El-Amraoui, Y. Messaddeq, and R. Vallee, "3.77 μm fiber laser based on cascaded Raman gain in a chalcogenide glass fiber," *Opt. Lett.*, vol. 39, no. 7, pp. 2052–2055, Apr. 2014.
- [4] P. P. Jiang *et al.*, "High power Yb fiber laser with picosecond bursts and the quasi-synchronously pumping for efficient midinfrared laser generation in optical parametric oscillator," *IEEE Photon. J.*, vol. 8, no. 3, Jun. 2016, Art. no. 1501807.
- [5] X. B. Wei *et al.*, "110 W 1678 nm laser based on high-efficiency optical parametric interactions pumped by high-power slab laser," *Opt. Lett.*, vol. 41, no. 7, pp. 1608–1611, Apr. 2016.
- [6] V. Kemlin *et al.*, "Widely tunable optical parametric oscillator in a 5 mm thick 5% MgO:PPLN partial cylinder," *Opt. Lett.*, vol. 38, no. 6, pp. 860–862, Mar. 2013.
- [7] S. Mieth, A. Henderson, and T. Halfmann, "Tunable, continuous-wave optical parametric oscillator with more than 1 W output power in the orange visible spectrum," *Opt. Exp.*, vol. 22, no. 9, pp. 11182–11191, May 2014.
- [8] M. Siltanen, M. Vainio, and L. Halonen, "Pump-tunable continuous-wave singly resonant optical parametric oscillator from 2.5 to 4.4 μm ," *Opt. Exp.*, vol. 18, no. 13, pp. 14087–14092, Jun. 2010.

- [9] S. Chaitanya Kumar, R. Das, G. K. Samanta, and M. Ebrahim-Zadeh, "Optimally-output-coupled, 17.5 W, fiber-laser-pumped continuous-wave optical parametric oscillator," *Appl. Phys. B*, vol. 102, no. 1, pp. 31–35, Jan. 2011.
- [10] H. Taniguchi, S. Yamamoto, and Y. Hirano, "High-average power optical parametric oscillator based on PPMgLN," *Mitsubishi Cable Industries Rev.*, vol. 98, pp. 88–91, Oct. 2001.
- [11] Y. F. Peng, W. M. Wang, X. B. Wei, and D. M. Li, "High-efficiency mid-infrared optical parametric oscillator based on PPMgO: CLN," *Opt. Lett.*, vol. 34, no. 19, pp. 2897–2899, Oct. 2009.
- [12] P. Zeil, N. Thilmann, V. Pasiskevicius, and F. Laurell, "High-power, single-frequency, continuous-wave optical parametric oscillator employing a variable reflectivity volume Bragg grating," *Opt. Exp.*, vol. 22, no. 24, pp. 29907–29913, Dec. 2014.
- [13] Y. F. Peng, X. B. Wei, W. M. Wang, and D. M. Li, "High-power 3.8 μm tunable optical parametric oscillator based on PPMgO: CLN," *Opt. Commun.*, vol. 283, no. 20, pp. 4032–4035, Oct. 2010.
- [14] T. L. Zhang *et al.*, "Widely tunable, high-repetition-rate, dual signal-wave optical parametric oscillator by using two periodically poled crystals," *Opt. Commun.*, vol. 272, no. 1, pp. 111–115, Jan. 2007.
- [15] I. Breunig, R. Sowade, and K. Buse, "Limitations of the tunability of dual-crystal optical parametric oscillators," *Opt. Lett.*, vol. 32, no. 11, pp. 1450–1452, Jun. 2007.
- [16] Y. J. Yu *et al.*, "Experimental study of multiple optical parametric oscillator based on MgO:APLN and its evolution analysis of back conversion," *Acta Phys. Sin.*, vol. 64, no. 4, Feb. 2015, Art. no. 044203.
- [17] B. Y. Gu, B. Z. Dong, Y. Zhang, and G. Z. Yang, "Enhanced harmonic generation in aperiodic optical superlattices," *Appl. Phys. Lett.*, vol. 75, no. 15, pp. 2175–2177, Oct. 1999.
- [18] F. Wu, X. F. Chen, X. L. Zeng, Y. P. Chen, and Y. X. Xia, "Generation of multi-wavelength light sources for optical communications in aperiodic optical superlattice," *Chin. Opt. Lett.*, vol. 3, no. 12, pp. 708–711, Dec. 2005.
- [19] O. Paul *et al.*, "Temperature-dependent Sellmeier equation in the MIR for the extraordinary refractive index of 5% MgO doped congruent LiNbO₃," *Appl. Phys. B*, vol. 86, no. 1, pp. 111–115, Jan. 2007.
- [20] F. Song *et al.*, "Determination of thermal focal length and pumping radius in gain medium in laser-diode-pumped Nd: YVO₄ lasers," *Appl. Phys. Lett.*, vol. 81, no. 12, pp. 2145–2147, Sep. 2002.
- [21] Q. Sheng *et al.*, "Continuous-wave intra-cavity singly resonant optical parametric oscillator with resonant wave output coupling," *Opt. Exp.*, vol. 20, no. 25, pp. 27953–27958, Dec. 2012.
- [22] G. A. Turnbull, M. H. Dunn, and M. Ebrahimzadeh, "Continuous-wave, intracavity optical parametric oscillators: An analysis of power characteristics," *Appl. Phys. B*, vol. 66, no. 6, pp. 701–710, Jun. 1998.